Am J Physiol Endocrinol Metab 283: E390–E401, 2002.
First published February 26, 2002; 10.1152/ajpendo.00428.2001.

New creatine transporter assay and identification of distinct creatine transporter isoforms in muscle

BERND WALZEL,[1*] OLIVER SPEER,[1*] ERNIE BOEHM,[3] SØREN KRISTIANSEN,[2] SHARON CHAN,[4] KIERIAN CLARKE,[4] JOSEPH P. MAGYAR,[1] ERIK A. RICHTER,[2] AND THEO WALLIMANN[1]

[1]*Institute of Cell Biology, Eidgenössische Technische Hochschule-Zurich, Hönggerberg, CH-8093 Zurich, Switzerland;* [2]*Human Physiology, Copenhagen Muscle Research Center, Institute of Exercise and Sport Sciences, University of Copenhagen, DK-2100 Copenhagen Ø, Denmark;* [3]*Wellcome Trust Centre for Human Genetics, Oxford OX3 7BN; and* [4]*Department of Biochemistry, University of Oxford, Oxford OX1 3QU, United Kingdom*

Received 24 September 2001; accepted in final form 14 February 2002

Walzel, Bernd, Oliver Speer, Ernie Boehm, Søren Kristiansen, Sharon Chan, Kierian Clarke, Joseph P. Magyar, Erik A. Richter, and Theo Wallimann. New creatine transporter assay and identification of distinct creatine transporter isoforms in muscle. *Am J Physiol Endocrinol Metab* 283: E390–E401, 2002. First published February 26, 2002; 10.1152/ajpendo.00428.2001.—Despite the pivotal role of creatine (Cr) and phosphocreatine (PCr) in muscle metabolism, relatively little is known about sarcolemmal creatine transport, creatine transporter (CRT) isoforms, and subcellular localization of the CRT proteins. To be able to quantify creatine transport across the sarcolemma, we have developed a new in vitro assay using rat sarcolemmal giant vesicles. The rat giant sarcolemmal vesicle assay reveals the presence of a specific high-affinity and saturable transport system for Cr in the sarcolemma (Michaelis-Menten constant 52.4 ± 9.4 μM and maximal velocity value 17.3 ± 3.1 pmol·min^{-1}·mg vesicle protein^{-1}), which cotransports Cr into skeletal muscle together with Na^+ and Cl^- ions. The regulation of Cr transport in giant vesicles by substrates, analogs, and inhibitors, as well as by phorbol 12-myristate 13-acetate and insulin, was studied. Two antibodies raised against COOH- and NH_2-terminal synthetic peptides of CRT sequences both recognize two major polypeptides on Western blots with apparent molecular masses of 70 and 55 kDa, respectively. The highest CRT expression occurs in heart, brain, and kidney, and although creatine kinase is absent in liver cells, CRT is also found in this tissue. Surprisingly, immunofluorescence staining of cultured adult rat heart cardiomyocytes with specific anti-CRT antibodies, as well as cell fractionation and cell surface biotinylation studies, revealed that only a minor CRT species with an intermediate molecular mass of ~58 kDa is present in the sarcolemma, whereas the previously identified major CRT-related protein species of 70 and 55 kDa are specifically located in mitochondria. Our studies indicate that mitochondria may represent a major compartment of CRT localization, thus providing a new aspect to the current debate about the existence and whereabouts of intracellular Cr and PCr compartments that have been inferred from [^{14}C]PCr/Cr measurements in vivo as well as from recent in vivo NMR studies.

plasma membrane giant vesicles; sarcolemma; mitochondria; subcellular compartmentation of creatine; bioenergetics

CLINICAL APPLICATIONS OF CREATINE (Cr) supplementation have recently attracted considerable attention, and a series of intriguing new discoveries about potential therapeutic effects of Cr have been made. Cr analogs have been proven to be prospective anticancer agents that act synergistically with currently used chemotherapeutics (3, 25, 35–37, 53), and beneficial effects of Cr supplementation have been reported for congestive heart failure (17, 26), atherosclerotic heart disease (8, 12, 44), neuromuscular disease (38, 64, 62), stroke, and neurodegenerative disease (7, 30, 39), as well as in the treatment of muscular weakness in gyrate atrophy (22, 56, 68), as a therapeutic aid for Duchenne muscular dystrophy (45, 48, 75) and mitochondrial myopathies (31) (see Refs. 65, 77 for review). Apparently, many skeletal muscle and heart diseases are associated with disturbances in Cr metabolism, either as a primary defect or secondary to other metabolic derangements that critically influence skeletal muscle performance. The reduced intramuscular Cr and phosphocreatine (PCr) content that is observed in such diseases seems to be related to a decreased expression and/or accumulation of the Cr transporter (CRT) that is responsible for Cr uptake and storage in these cell types (43, 63). Muscle diseases with impaired ion regulation such as Duchenne muscular dystrophy, where the ionic balance, especially Ca^{2+} homeostasis, is disturbed, may contribute to the dysfunction of the CRT, which relies on a sodium chloride gradient to cotransport Cr across the plasma membrane (21).

CRT has been mapped to the human chromosome Xq28 (13, 27), a locus that has been linked to several hereditary neuromuscular disorders such as Barth syndrome and infantile cardiomyopathy (1, 4). Because

* These authors contributed equally to this study.

Address for reprint requests and other correspondence: T. Wallimann, Institute of Cell Biology, ETH-Hönggerberg HPM F42, CH-8093 Zurich, Switzerland (E-mail: theo.wallimann@cell.biol.ethz.ch).

The costs of publication of this article were defrayed in part by the payment of page charges. The article must therefore be hereby marked "*advertisement*" in accordance with 18 U.S.C. Section 1734 solely to indicate this fact.

of the major role of Cr in muscular physiology, we consider the CRT a candidate gene that may be involved or is affected in these diseases. Indeed, very recently, a CRT gene defect has been described that leads to a Cr deficiency syndrome with developmental delay, hypotonia, and severe delay in both speech and expressive language function (51).

Given the importance of Cr supplementation in pathology, it seems very surprising that there is no in vitro assay available to study possible functional impairments of the CRT in such diseases. The CRT assay described here, as well as the anti-CRT antibodies characterized in this study, may prove useful for functional testing and clinical screening of such patients, respectively.

The expression of the CRT in several tissues has been studied earlier with the use of specific anti-CRT antibodies (20, 41, 43, 66) and has revealed different forms of CRT, expressed in various tissues, that are most likely derived from alternative splicing (20). The finding of two different mRNAs in these tissues (21, 23, 42, 52, 55) has supported this assumption.

Here, using our anti-CRT antibodies generated against both NH_2- and COOH-terminal peptides, we provide evidence for the existence of independent forms of CRT species in skeletal muscle. In combination with in situ biotinylation and immunofluorescence methods, a minor CRT species present in the sarcolemma and two major, yet unknown, CRT species specifically located in mitochondria are revealed.

EXPERIMENTAL PROCEDURES

Materials. Nycodenz, collagenase (type VII), β-guanidinopropionic acid (β-GPA), guanidinoacetic acid (GAA), Cr, cyclocreatine, creatinine, taurine, PCr, ouabain, gramicidin A, phorbol 12-myristate 13-acetate (PMA), 4α-phorbol 12,13-didecanoate, anti-protease cocktail, avidin, and streptavidin beads were from Sigma (Buchs, Switzerland); Phenylmethylsulfonyl fluoride (PMSF) was from SERVA (Heidelberg, Germany); [4-^{14}C]Cr was from American Radiolabeled Chemicals; [^{3}H]mannitol was from NEN Life Science (The Netherlands); Hybond-P polyvinylidene difluoride (PVDF) membrane, Percoll, and ECL-Plus chemiluminescence detection kit were from Amersham Biosciences (Dübendorf, Switzerland). Secondary antibodies goat anti-mouse Cy5 and goat anti-rabbit Cy3 were from Amersham Biosciences, goat anti-rabbit FITC and monkey anti-sheep FITC were from Pierce, and goat anti-rabbit horseradish peroxidase (HRP) was from Nordic (Tilburg, The Netherlands). Primary antibodies: monoclonal mouse anti-voltage-dependent anion channel (VDAC) was from Calbiochem (USA), COOH- and NH_2-terminal polyclonal CRT antipeptide antibodies were produced as described (20), polyclonal adenine nucleotide translocase (ANT) antipeptide antibodies were produced as described (50), mouse anti-cytochrome *c* oxidase subunit IV (COX) was from Molecular Probes, polyclonal sheep anti-CRT antibodies were produced by ANAWA (Wangen, Switzerland), and their specificity against CRT protein has been established (unpublished observations), polyclonal anti-human sarcomeric mitochondrial creatine kinase (Mi_s-CK) antibody (32) and polyclonal anti-human cytosolic muscle-type (M)-CK antibody (54) have been described.

Cr transport assay into giant sarcolemmal vesicles. Preparation and characterization of giant sarcolemmal vesicles from rat skeletal muscles (gastrocnemius, soleus, and quadriceps femoris) were performed as described (34, 46). The purity of the vesicle preparation was additionally supported by Western blotting with the use of antibodies against the Na^+-K^+-ATPase and the mitochondrial markers VDAC and ANT (data not shown). The protein concentration of the vesicle preparation was adjusted to 5 mg/ml. Cr transport was measured at 37°C and started by adding 10 μl of the vesicle preparation to 90 μl of transport buffer. The transport buffer contained 10 μM [^{14}C]Cr, 1 μCi/ml [^{3}H]mannitol, 100 μM Cr, 134 mM NaCl, 2 mM $MgCl_2$, 2 mM Na_2HPO_4, and 10 mM Tris·HCl, pH 7.4. To determine the ion dependence, 134 mM NaCl was exchanged either by 134 mM KCl, LiCl, NaF, or Na-acetate or Na-citrate or 88 mM Na_2SO_4. Inhibition of Cr transport was measured in NaCl transport buffer with final concentrations of 4 mM of glucose, fructose, or maltose or 1 mM each of either ouabain, β-GPA, GAA, PCr, creatinine, cyclocreatine, taurine, or caffeine or 1 μM gramicidin A or 10 μM of either PMA or 4α-phorbol 12,13-didecanoate as 100-fold stock solutions in ethanol. In the experiments designed to study the effects of insulin on vesicle transport of Cr, anesthetized rats were injected with 10 U of human insulin (Novo Nordisk) in a tail vein 20 min before muscles were removed for the preparation of giant vesicles, as described (46). The transport assay was stopped by adding 1 ml of ice-cold transport buffer (lacking isotopes and Cr), centrifugation at 16,000 *g* for 1 min, and removal of the supernatant. The pellet was solubilized in 100 μl of 1% SDS and counted in 4 ml of the scintillation cocktail Ultima Gold XR (Packard) in a Packard 1500 Tri-Carb liquid scintillation counter. Double-isotope measurement settings were 0–18 eV for the ^{3}H isotope and 18–256 eV for the ^{14}C isotope.

Protein extracts from rat tissues. Wistar rats (male, 3–4 mo of age) were anesthetized with diethyl ether and killed by cervical dislocation. Tissues were freed from fat and connective tissue, washed in MSH buffer (10 mM HEPES-HCl, pH 7.4, 220 mM mannitol, 70 mM sucrose) and homogenized in 5 vol of MSH at 0°C. Brain, kidney, testis, and nonperfused liver were homogenized with a glass Teflon potter, whereas intestine, lung, and muscle tissues were homogenized with a Polytron mixer. The homogenate was supplemented to 5% SDS and heated at 75°C for 15 min with shaking. After centrifugation at 16,000 *g* for 10 min, the supernatant was used for analysis. Protein determination was performed with bicinchoninic acid (BCA) protein assay reagent from Pierce. SDS-PAGE minigels were carried out according to standard procedures with 30 μg protein/lane. Immunoblots were performed using COOH- or NH_2-terminal anti-CRT antibody.

Tissue extracts and isolation of mitochondria from rat soleus. Wistar rats (male, 3–4 mo of age) were anesthetized with diethyl ether and killed by cervical dislocation. Soleus muscle was immediately homogenized by a Polytron mixer in 40 ml of HEPES-sucrose buffer containing 250 mM sucrose, 10 mM HEPES-KOH, pH 7.4, 0.5% BSA (essentially fat free) and 1 mM EDTA. The homogenate was centrifuged for 10 min at 700 *g* to remove heavy debris such as platelets and nuclei. An aliquot from the supernatant was taken as tissue extract. The supernatant was centrifuged for 10 min at 7,000 *g*. The supernatant was taken as cytoplasm, and the pellet containing mitochondria was resuspended in 60 ml of 250 mM sucrose, 10 mM HEPES-KOH, pH 7.4, 100 μM EGTA, and 25% Percoll and centrifuged for 35 min at 100,000 *g*. Percoll fractions containing highly enriched mitochondria were washed twice with 250 mM sucrose, 10 mM HEPES-KOH, pH 7.4, and 100 μM EGTA at 7,000 *g* for 10 min.

Washed mitochondria were then recovered from the pellet and resuspended in 200 μl of buffer. Protein determination was performed with BCA protein assay reagent. SDS-PAGE minigels were carried out according to standard procedures with 10 μg protein/lane. Immunoblots were performed using COOH-terminal anti-CRT antibody, polyclonal anti-human Mi_s-CK antibody (as mitochondrial marker), and polyclonal anti-human M-CK antibody (as cytosolic marker).

Succinate dehydrogenase enzyme assay. The specific succinate dehydrogenase (SDH) activity of mitochondrial preparations was measured indirectly via the increase in the absorption of reduced cytochrome *c* at 550 nm ($\epsilon = 19\ mM^{-1}/cm$). Samples (10 μl) were incubated in 1 ml of 50 mM Na_2HPO_4, 50 mM NaH_2PO_4, pH 7.4, 100 μM cytochrome *c*, 1 mM KCN, and 2.5 mM succinate as described (5).

Cell cultures for immunofluorescence studies. For adult rat cardiomyocytes (ARC), ventricular cardiac myocytes of adult female rats (2 mo of age) were isolated by retrograde perfusion of hearts according to an established method (14). Culture dishes were coated with 0.1% gelatin. After isolation, ARC were cultured in M-199 medium containing 20% fetal calf serum, 20 mM Cr monohydrate, and 100 U/ml penicillin-streptomycin. For growth inhibition of fibroblasts and other proliferation-competent cells, 10 μM cytosine arabinoside was added to the medium.

Isolation of myocytes for cell surface labeling. Mouse cardiac myocytes were isolated according to established methods (47). Briefly, hearts from six control C57BL/10 mice (male, 6 mo of age) weighing ~30 g were excised under pentobarbitone anesthesia (140 mg/ml) and immediately arrested in perfusion buffer (see below). Hearts were perfused for 5 min by retrograde coronary perfusion with a calcium-free buffer containing (in mM) 134 NaCl, 5.4 KCl, 0.3 $NaH_2PO_4 \cdot 2H_2O$, 1.0 $MgCl_2$, 5.0 Na-acetate, 5.0 Na-pyruvate, 11 glucose, 5.0 HEPES, 20 taurine, and 10 Cr and 10 mU/ml insulin, pH 7.25. This was followed by 10 min with perfusion buffer supplemented with collagenase (1 mg/ml), protease (0.1 mg/ml), and $CaCl_2$ (80 μM). An increased coronary flow at 5–7 min indicated a breakdown of the coronary bed, at which point the coronary flow rate was reduced to 1 drop/s. Subsequently, the ventricles were dissected and placed in a stirred enzyme incubation solution (calcium-free buffer containing 1 mg/ml collagenase, 0.1 mg/ml protease, 10 mg/ml albumin, 100 μM $CaCl_2$) for 10 min at 37°C. The supernatant was filtered through a nylon gauze mesh and made up to 10 ml with wash solution (10 mg/ml albumin, 500 μM $CaCl_2$). Cells were centrifuged for 1 min at 20–30 *g* and resuspended again in 10 ml of wash solution.

Cell surface biotinylation. Cell surface expression of the CRT was determined using the membrane-impermeable biotinylation reagent sulfo-NHS-LC-biotin (10, 61). Isolated myocytes were washed three times with ice-cold PBS and then incubated with PBS containing 1.0 mg/ml sulfo-NHS-LC-biotin for 30–45 min with constant shaking at 4°C. After labeling, the cells were washed three times in ice-cold PBS containing glycine (15 mM) to quench the residual sulfo-NHS-LC-biotin. Subsequently, cells were solubilized by resuspension in solubilization buffer [containing 150 mM NaCl, 20 mM HEPES, 2 mM PMSF, 1 mM EDTA, 0.1% Triton X-100, and anti-protease cocktail (1:100 dilution)] and gentle shaking for ~1 h. The extracts were clarified by centrifugation at 13,000 *g* for 5 min at 4°C. A portion of the lysate was taken for immediate incubation with streptavidin beads, whereas the remaining lysate was kept for protein determination and immunoblotting of the total cell extract.

Streptavidin beads (100 μl) were washed three times in wash buffer (containing 150 mM NaCl and 10 mM Tris, pH 7.0) by rapid centrifugation. Lysate (100 μg protein) was added to the beads, incubated on ice, and rotated/shaken for 2 h. Samples were then washed by rapid centrifugation with wash buffer plus anti-proteases. To elute the biotinylated protein from the beads, 80 μl of urea buffer (containing 9 M urea, 2% SDS, and 100 mM Tris, pH 6.8) plus antiproteases were added and incubated (with constant shaking) for 30 min at 95°C. Finally, tubes were centrifuged at 13,000 *g*, and the supernatant representing the captured biotinylated protein was collected and subsequently analyzed by Western blotting.

Erythrocyte preparation. Fresh heparinized blood from mice (male, 6 mo of age) was taken and immediately spun at 13,000 *g* for 10 min. The supernatant was discarded, and red cells were washed by rapid centrifugation three times with isosmotic buffer (MOPS-buffered saline). The supernatant was discarded, and ~250 μl of red blood cells were resuspended in solubilization buffer (see *Cell surface biotinylation*) and incubated with shaking for 30 min at 4°C. The suspension was again spun at 13,000 *g* and the supernatant taken and kept at −70°C before use.

Western blotting. Total cell extracts (cardiac myocytes and erythrocytes at 20 and 100 μg protein/lane, respectively) and captured biotinylated proteins (100 μg protein/lane) were separated on a 10% SDS-polyacrylamide gel and subsequently transferred onto a Hybond-P PVDF membrane. The membrane was blocked with 5% fat-free milk powder in TBS-T buffer (137 mM NaCl, 2.6 mM KCl, 25 mM Tris·HCl, 0.1% Tween-20, pH 7.4) for 1 h at room temperature (followed by 1 h in TBS supplemented with avidin at a concentration of 20 μg/ml for the biotinylation experiments). After a 1-h washing, membranes were incubated with a 1:3,000 dilution of the anti-CRT COOH-terminal antibody for 1 h at room temperature. After a washing with TBS-T buffer, the blot was incubated with a 1:5,000 dilution of the HRP-conjugated anti-rabbit antibody. The immunoreactive bands were visualized using the ECL-Plus chemiluminescence detection kit.

Immunofluorescence of cultured adult rat myocytes and soleus sections. Freshly excised rat soleus muscle was fixed in PBS containing 3% paraformaldehyde. Tissues were embedded in paraffin and cut to 10-μm slices with a microtome. Paraffin was removed with xylole, and the slices were washed with 70% ethanol and stored in PBS. Cell cultures and sections of rat soleus were rinsed with PBS and then fixed with PBS and 0.3% PFA for 15 min at room temperature and washed three times for 5 min with PBS. After permeabilization with PBS and 0.3% Triton X-100 for 20 min at room temperature and washing for 3 × 5 min with PBS, the samples were blocked with PBS containing 4% milk powder for 1 h at room temperature. Finally, the samples were incubated with primary antibody at 4°C overnight. Antibody dilutions in PBS containing 4% milk powder were 1:200 for polyclonal rabbit anti-CRT COOH- or NH_2-terminal antibody, 1:100 for polyclonal sheep anti-CRT, 1:100 for polyclonal rabbit anti-ANT, 1:200 mouse anti-COX, and 1:50 for monoclonal mouse anti-VDAC. Controls were performed in parallel experiments with the use of the corresponding sera of nonimmunized animals, where no specific signal could be discerned (not shown). The cells were washed three times for 5 min with PBS followed by incubation with the conjugate dilutions in PBS for 2 h at room temperature (goat anti-rabbit FITC 1:200, goat anti-mouse Cy3 1:1,000, monkey anti-sheep FITC 1:200, goat anti-rabbit TRITC 1:200, goat anti-mouse Cy5 1:200). After three PBS washing steps of 5 min each, cells were embedded in antifading medium containing 30 mM Tris·HCl, pH 9.5, 70% (vol/vol) glycerol, and 240 mM *N*-propyl gallate and covered with coverslips. Sections were analyzed with a confocal microscope Zeiss Axio-

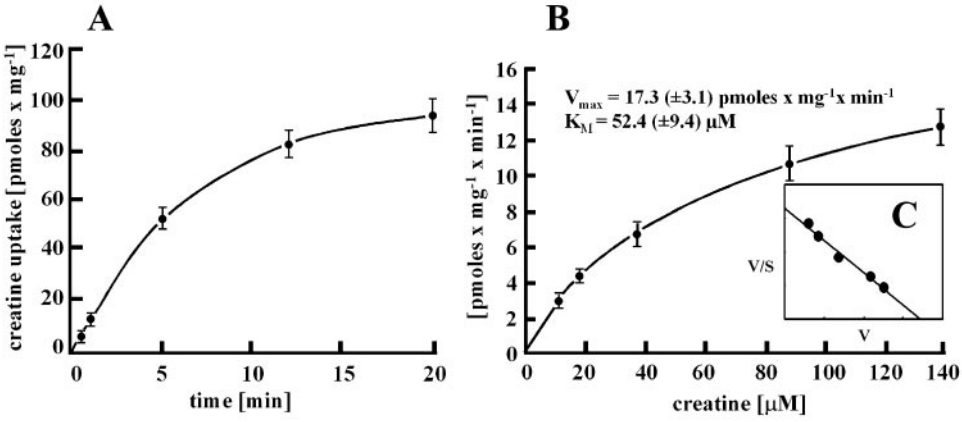

Fig. 1. Kinetics of sarcolemmal creatine (Cr) transporter (CRT). *A*: time course of Cr uptake into giant sarcolemmal vesicles measured at 100 μM Cr. Amount of Cr uptake is expressed as pmol/mg total vesicle protein. Values are means ± SE of 4 individual experiments, each measured in duplicate. *B*: initial rate of Cr uptake into giant sarcolemmal vesicles as a function of Cr concentration. Cr uptake was measured for 1 min at 11, 18, 38, 88, and 138 μM Cr, respectively. Velocity of Cr uptake is expressed as pmol·min^{-1}·mg^{-1} of total vesicle protein. Values are means ± SE of 4 individual experiments, in each of which Cr transport was measured in duplicate. *C*: uptake curve was fitted to Eadie Hofstee plot [transport velocity (V)/substrate concentration (S)] plotted against V. Michaelis-Menten constant (K_m) and maximal velocity (V_{max}) values (means ± SE) fitted from each individual uptake curve were 52.4 ± 9.4 μM and 17.3 ± 3.1 pmol·min^{-1}·mg^{-1} of vesicle protein, respectively.

phot fluorescence microscope, a Bio-Rad MRC-600 confocal scanner unit, and a Silicon Graphics Iris 4D/25 workstation. Images were recorded with oil immersion objectives using a Zeiss Neofluar ×40/1.3 objective or a Zeiss Neofluar ×63/1.3 objective. The system was equipped with an argon-krypton mixed-gas laser. Image processing was with a Silicon Graphics workstation using Imaris (Bitplane) software.

RESULTS

Characterization of Cr transport in sarcolemmal giant vesicles. The time course of Cr uptake into giant sarcolemmal vesicles (Fig. 1*A*) showed linear uptake until 5 min, whereupon leveling off occurred. Uptake in relation to concentration follows saturation kinetics with an apparent Michaelis-Menten constant (K_m) and maximal velocity (V_{max}) for Cr transport of 52.4 ± 9.4 μM and 17.3 ± 3.1 pmol·min^{-1}·mg^{-1} vesicle protein, respectively (Fig. 1, *B* and *C*).

Cr transport into skeletal muscle was dependent on an extracellular Na^+ and Cl^- gradient. As shown in Fig. 2, replacement of the NaCl gradient by a potassium or lithium chloride gradient in the extravesicular medium completely abolished Cr transport. Likewise, the presence of 1 μM gramicidin A, a powerful Na^+ ionophore that completely collapses the Na^+ gradient between extra vs. intravesicular space (69), stopped the Cr transport due to Na^+ influx into the vesicles (Table 1). In contrast, ouabain, a selective inhibitor of the Na^+-K^+-ATPase pump (11, 57), the enzyme that establishes the sodium gradient in intact cells in vivo and balances the influx and efflux of sodium and potassium cations, was unable to affect Cr uptake (Table 1).

In addition, the effects of changes in the external concentrations of anions on Cr uptake into skeletal muscle were examined. Figure 2 also shows that Cr transport considerably diminished when uptake buffers containing anions other than Cl^- were used. Exchange of the NaCl gradient by an Na-fluoride, -citrate, -acetate, or -sulfate gradient led to a significant loss of Cr transport activity. Thus Cr uptake into skeletal muscle appears to be strictly dependent on an NaCl gradient.

To analyze the specificity of the sarcolemmal CRT for its substrate Cr, we examined the effects of structurally related compounds and Cr analogs for their ability to inhibit and/or compete with the CRT activity. Figure 3 shows that β-GPA, a well known competitive inhibitor of Cr uptake (16), had the most prominent inhibitory effect on Cr transport into skeletal muscle. The presence of 1 mM β-GPA in the extravesicular buffer was sufficient to decrease Cr uptake to ~25% of control rates. The Cr analog cyclocreatine, at 1 mM in the

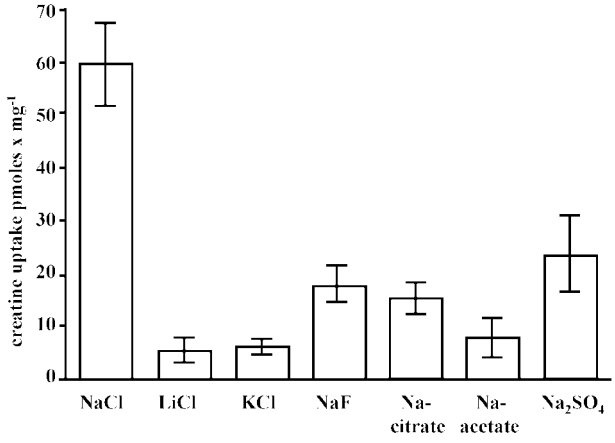

Fig. 2. Ion dependence of Cr uptake into giant sarcolemmal vesicles. Cr uptake assays were performed for 5 min at 100 μM Cr in uptake buffers containing 132 mM of the salts indicated, except for Na_2SO_4, which was 88 mM. Amount of Cr uptake is expressed as pmol/mg total vesicle protein. Values are means ± SE of 4 individual experiments, each measured in duplicate.

Table 1. *Cr uptake into giant sarcolemmal vesicles in the presence of various effectors*

	Assay Concentration	Creatine Uptake into Giant Sarcolemmal Vesicles, pmol·mg^{-1}·5 min^{-1}
Standard assay		58.75 ± 4.31
Standard assay + ethanol*		54.75 ± 5.24
Ouabain*	1 mM	57.96 ± 4.27
Gramicidin A*	1 μM	5.12 ± 1.65
Phorbol 12-myristate 13-acetate*	10 μM	54.88 ± 5.65
4α-Phorbol 12,13-didecanoate*	10 μM	58.45 ± 3.02
Caffeine	1 mM	62.18 ± 6.10
Glucose	4 mM	59.70 ± 1.06
Fructose	4 mM	56.35 ± 6.63
Maltose	4 mM	60.01 ± 2.22
Insulin	10 U	55.09 ± 3.94

Values are means ± SE. Creatine (Cr) uptake assays were performed for 5 min at 100 μM Cr in uptake buffers containing the compounds indicated or after additional preincubation (*) for 20 min at 37°C at the indicated concentration. Insulin was intravenously injected into rats 20 min before muscles were removed for vesicle preparation. Amount of Cr uptake is expressed as pmol/mg total vesicle protein. Mean values are from 4 individual experiments, in each of which Cr transport was measured in duplicate.

transport buffer, led to an ~50% decrease in Cr uptake, indicating that it competes for the CRT and is itself taken up by the giant sarcolemmal vesicles. Other structurally related compounds such as creatinine, the degradation product of Cr, and taurine did not inhibit Cr uptake to any significant level, whereas GAA, the precursor molecule of Cr, decreased Cr uptake by ~15%. Remarkably, the phosphorylated form of Cr was not recognized as a substrate of the CRT and did not interfere with Cr uptake (Fig. 3).

We further studied the effect of caffeine, which was shown to somehow attenuate the ergogenic effects of Cr (67) on Cr uptake, but we were not able to show direct effects of this drug on Cr uptake at concentrations of 1 mM in the transport buffer and after preincubation of the vesicle preparation for 20 min at 37°C (Table 1).

Active and inactive phorbol esters, which were used in other studies to single out the regulation of CRT activity by protein kinase C (PKC)-dependent phosphorylation (9, 42), were not able to influence Cr transport activity in giant sarcolemmal vesicles when present in the transport buffer and after preincubation of the vesicle preparation with these compounds for 20 min at 37°C at 10 μM concentration (Table 1). Also the carbohydrates glucose, fructose, and maltose could not change Cr uptake into giant vesicles by its presence in the transport buffer (Table 1). Likewise insulin, after intravenous injection into rats and subsequent preparation of giant vesicles, did not result in significant alterations of Cr transport compared with vesicle preparations from control animals (Table 1).

Expression of CRT polypeptide species in different tissues. To find out whether Cr content correlates with CRT expression in various tissues, we generated specific antipeptide antibodies directed against the COOH- and NH_2-terminal regions of the cDNA-derived CRT sequence (20). Neither region shows any sequence homology to other members of the Na^+- and Cl^--dependent neurotransmitter transporter family or to any other proteins in a homology search in the EMBL database. On immunoblots, with the use of these antisera, two major protein bands with an apparent electrophoretic mobility of 70 and 55 kDa were consistently recognized in all tissues tested (Fig. 4*A*; only the COOH-terminal antibody shown). Protein expression was most prominent in excitable and metabolically active tissues such as brain and heart, as well as in kidney, and also in liver, the principal organ where the final step of Cr synthesis takes place. Lower levels of CRT expression were observed in white glycolytic skeletal muscle (gastrocnemius), lung, testis, and intestine.

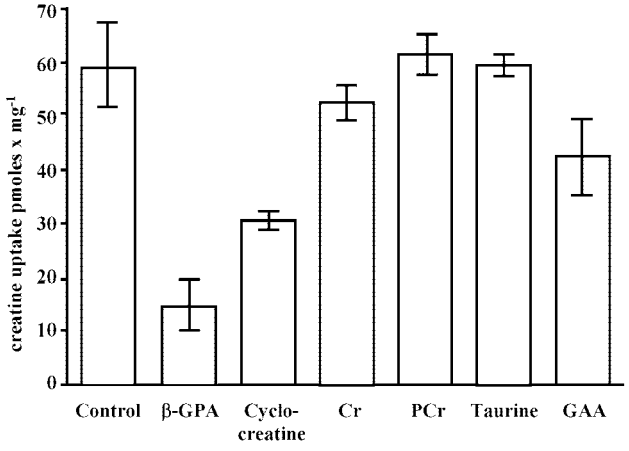

Fig. 3. Inhibition of Cr uptake into giant sarcolemmal vesicles by structural analogs of Cr. Cr uptake assays were performed for 5 min at 100 μM Cr in uptake buffers containing 132 mM NaCl (control) and 1 mM of the compounds indicated. β-GPA, β-guanidinopropionic acid; BAA, guanidinoacetic acid; PCr, phosphocreatine. Velocity of Cr uptake is expressed as pmol/mg total vesicle protein. Values are means ± SE of 4 individual experiments, each measured in duplicate.

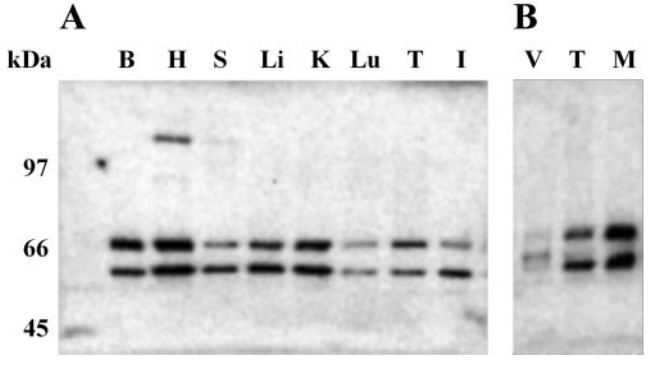

Fig. 4. Representative immunoblot of CRT protein in total tissue extracts or cell fractions thereof (30 μg of protein loaded/lane). *A*: total tissue extracts from rat brain (B), heart (H), gastrocnemius muscle (S), liver (Li), kidney (K), lung (Lu), testis (T), and intestine (I). *B*: giant sarcolemmal vesicles obtained from rat skeletal muscle (V), from a total protein extract of rat soleus muscle (T), and from highly purified mitochondria obtained by ion fractionation and density gradient centrifugation of rat soleus muscle (M).

Differential subcellular compartmentation of CRT polypeptide species. CRT protein is expected to be highly enriched in purified plasma membrane vesicles. However, anti-CRT immunoblots of giant vesicles (Fig. 4*B*, *lane V*) showed only minor expression of an ~58-kDa protein taking a total protein extract from rat skeletal muscle (Fig. 4*B*, *lane T*) as reference. The immunoreactive signal of the 55- and 70-kDa proteins was almost absent, whereas a rather weak 58-kDa polypeptide appeared that was enriched in these giant vesicle preparations (Fig. 4*B*, *lane V*). On the other hand, a preparation of purified mitochondria from rat skeletal muscle showed an enrichment of the 55- and 70-kDa CRT immunoreactive bands compared with the total extract (Fig. 4*B*, *lane M*).

This result was confirmed by cell fractionation of rat soleus muscle and purification of mitochondria in Percoll density gradients (Fig. 5). The purity of the mitochondrial fraction was carefully checked with cytosolic and mitochondrial marker antibodies anti-MCK and anti-Mi_s-CK, respectively, showing a high enrichment of CRT proteins in the mitochondrial preparation (Fig. 5, *A* and *B*). Furthermore, the purity of the mitochondrial preparations was controlled by measuring enzyme activities of complex II (SDH) and complex III (cytochrome *c* reductase) indirectly via increasing absorption of reduced cytochrome *c*.

The relative surface abundance of the CRT from cardiac myocytes was determined using a surface biotinylation study, which proves that the third ~58-kDa polypeptide band, which is seen in the giant sarcolemmal vesicles, binds to the streptavidin beads (Fig. 6*A*, *lanes 1* and *3*) and consequently appears to be located on the cell surface. In contrast, the 55- and 70-kDa CRT immunoreactive bands seen in the total extract (Fig. 6*A*, *lanes 2* and *4*) and in the total extracts of Fig. 4*A* of all tissues tested could not be discerned by cell surface labeling.

In addition, erythrocytes from mouse, which were shown to possess an active NaCl-dependent CRT (2) but do not contain mitochondria, were probed for CRT expression. We found that erythrocytes from mouse express only a single ~58-kDa polypeptide form of the CRT (Fig. 6*B*) with an apparently similar electrophoretic mobility as that found in the captured biotinylated protein and in the giant sarcolemmal vesicle preparations. There was no sign of the presence of polypeptides at 55 or 70 kDa.

Indirect immunofluorescence labeling of cultured adult rat cardiomyocytes with anti-CRT antibodies clearly shows co-staining of anti-CRT signal with mitochondrial marker antibodies directed against ANT or VDAC (Fig. 7, *A-D*). This result was also obtained by immunofluorescence studies on cross sections of rat soleus muscle by use of anti-CRT antibodies, with anti-COX antibodies as mitochondrial marker (Fig. 7, *E-H*). Because the immunofluorescence signal from the subsarcolemmal mitochondria is very strong, the weak plasma membrane staining in soleus cross sections overlapping with sarcolemma-associated mitochondria often cannot be clearly discerned.

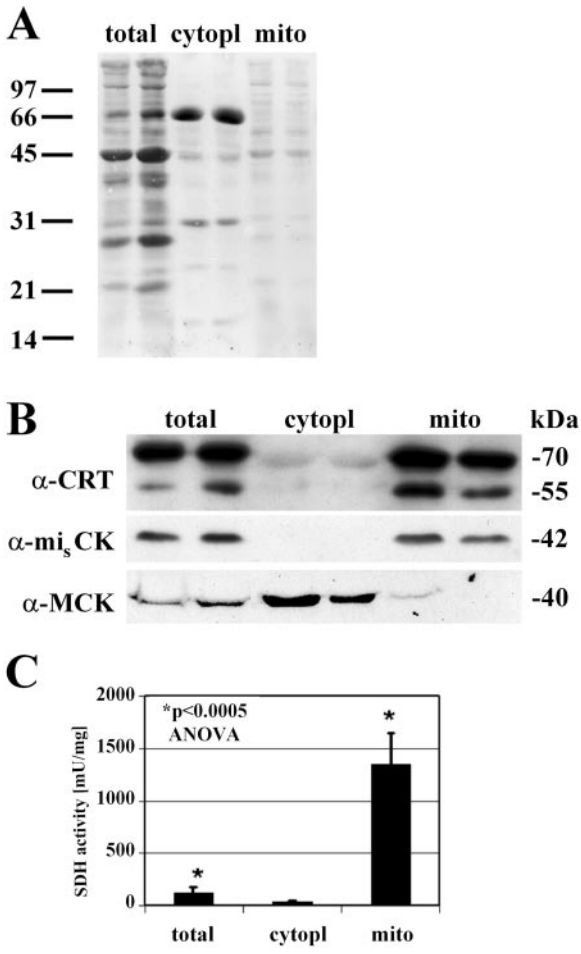

Fig. 5. Identification of CRT in rat soleus mitochondria. Ten micrograms each of total tissue extract (total) of rat soleus muscle, together with the corresponding cytoplasmic fractions (cytopl) and mitochondria (mito), isolated from adult rat soleus muscle, were electroblotted, stained with 0.2% Ponceau red in 3% trichloroacetic acid solution (*A*) and probed with polyclonal rabbit anti-CRT antibody and a polyclonal anti-human sarcomeric mitochondrial creatine kinase (Mi_s-CK), which is located in the mitochondrial intermembrane and intercristae membrane space and is also concentrated in contact sites (thus used as mitochondrial enzyme marker), as well as with polyclonal anti-human cytosolic muscle-type (M)-CK antibody (as cytosolic enzyme marker). Shown are the extracts from two different animals (*A* and *B*). Both the 55- and 70-kDa bands were stained equally with anti-COOH- (shown here) and anti-NH_2-terminal antibodies (not shown). To check the mitochondrial preparations, the enzyme activities of complex II [succinate dehydrogenase (SDH)] and complex III (cytochrome *c* reductase) were measured indirectly via increasing absorption of reduced cytochrome *c*. Complex IV [cytochrome *c* oxidase (COX)] was blocked with 1 mM KCN to keep cytochrome *c* reduced. Electrons were fed in with 2.5 mM succinate. Soleus muscle fractions from 3 animals were measured in triplicate. The means of the total extract and the mitochondrial fraction are statistically significantly different ($P < 0.0005$, one-way ANOVA; *C*).

The Cr transport studies presented here for determining the kinetics of CRT were routinely done with sarcolemma vesicles isolated from anesthetized rats kept on a normal rat feed diet. However, to address the question of whether CRT expression in the plasma membrane could possibly be altered by the extracellular availability of Cr, we were looking for a possible increase in CRT expression in the plasma membrane of

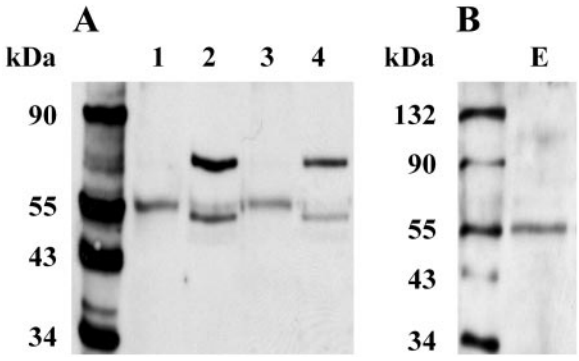

Fig. 6. *A*: representative immunoblot of CRT protein from captured biotinylated protein samples and total detergent extracts of mouse cardiomyocytes. *Lanes 1* and *3* contain streptavidin-separated biotin-labeled protein (100 μg protein/lane). *Lanes 2* and *4* contain whole cell lysates (20 μg protein/lane). Only one ~58-kDa immunoreactive band of the CRT is recognized by the CRT antibody in the biotinylated samples, which represents the sarcolemmal fraction of the cardiomyocyte. In contrast, the whole cell lysate shows 2 characteristic immunoreactive bands at 55 and 70 kDa, respectively. *Lanes 1* and *2*, as well as *lanes 3* and *4*, represent cardiomyocyte extracts from 2 separate mice. *B*: representative immunoblot of CRT protein from whole erythrocyte cell lysates of mouse. Only one ~58-kDa band of the CRT is recognized by the antibody in the erythrocyte.

ARC cultured in either Cr-deficient or Cr-supplemented medium for ≤10 days. Even under Cr-deficient conditions, where ARC start to display abnormally long and enlarged mitochondria with paracrystalline intramitochondrial inclusions (15), we did not observe an increase in sarcolemmal immunofluorescence signal in such ARC (not shown).

DISCUSSION

A new in vitro assay: Cr transport into giant sarcolemmal vesicles. Many skeletal muscle, heart, and neuromuscular diseases are characterized by a reduced intracellular Cr and PCr content, and Cr supplementation, which increases Cr content in skeletal muscle ≤20%, has been reported to be beneficial in the treatment of these diseases (77). In addition, the CRT gene has been mapped to the human chromosome Xq28 (13, 27), a locus that has been linked to several neuromuscular diseases (1, 4). Thus the sarcolemmal CRT, which regulates intracellular Cr content and is responsible for maintaining the extremely high concentration gradient across the plasma membrane, is a likely candidate gene that may be functionally affected by, or is even responsible for, some of these diseases, as has been already demonstrated in patients with Cr deficiency syndrome (51). However, research to study a possible involvement of the CRT in such diseases, i.e., due to mutations leading to the expression of a nonfunctional protein, has been hampered by the lack of a suitable assay system that would allow the comparison of the CRT parameters in healthy and pathological subjects. Because the preparation of giant sarcolemmal

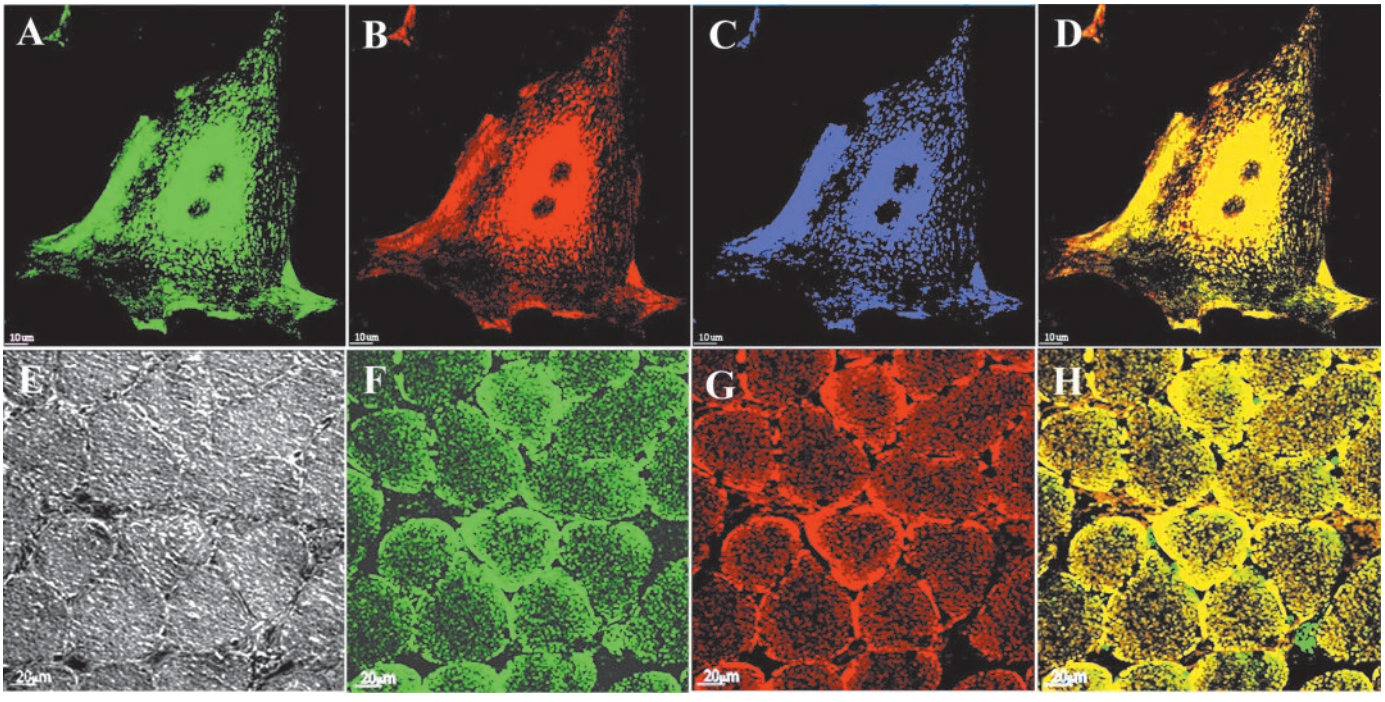

Fig. 7. Representative confocal microscopic images of a single cultured adult rat cardiomyocyte (*A-D*) and of cross sections of rat soleus (*E-H*). Indirect anti-CRT immunofluorescence staining (*A*) was co-stained for the mitochondrial marker proteins adenine nucleotide translocase (ANT; *B*) and voltage-dependent ion channel (VDAC; *C*). Areas of co-localization of CRT immunofluorescence with ANT signal are specified in yellow (*D*). Phase contrast image of cross sections of rat soleus (*E*) and indirect anti-CRT immunofluorescence staining (*F*) co-stained for the mitochondrial marker protein COX (*G*). Areas of co-localization of CRT immunofluorescence with mitochondria are specified in yellow (*H*). Note, staining shown here was with anti-COOH-terminal anti-CRT antibody, but the same results were obtained using anti-NH_2-terminal anti-CRT antibodies (not shown).

vesicles from human biopsies has already been studied in the case of the lactate transporter (28, 29) and GLUT4 (34), the Cr transport assay described here may provide a novel tool to investigate a possible involvement of the CRT in such diseases.

Skeletal muscle CRT from rat, present in the giant sarcolemmal vesicles, clearly showed a specific, saturable, high-affinity, and NaCl-dependent uptake of Cr, which is best inhibited by the Cr analogs β-GPA and cyclocreatine. The apparent K_m of 52 μM, as measured here, is well in agreement with that of earlier studies (77) that investigated the kinetic parameters of the CRT and thus seems to reflect the physiologically very low Cr plasma levels of 25–50 μM (70, 77).

As shown in Fig. 3, the phosphorylated form of Cr is not a substrate for the CRT. Consequently, the intracellular formation of PCr by the PCr/CK system, as well as the strict discrimination between Cr and PCr by the CRT, leads to entrapment of PCr inside the cell, since PCr escapes equilibration. This thermodynamically facilitates further Cr uptake and helps maintain the enormous total Cr concentration gradient (600- to 1,000-fold) across the plasma membrane. The V_{max} of Cr uptake into giant sarcolemmal vesicles is somewhat difficult to compare with previous studies of the CRT, with either intact muscle or myogenic cells, since these values are given relative to different measures of tissue mass, intracellular water volume, tissue dry weight, or mass of protein. When the V_{max} is compared with other plasma membrane transporters such as GLUT4 (46) or lactate transporter (29), which were investigated using sarcolemmal giant vesicles, Cr uptake seems slow. In view of the physiological function of a sarcolemmal CRT, that is, to transport as much Cr into the muscle cells as has been lost by the slow and constant nonenzymatic degradation of Cr to creatinine, Cr turnover rates are expected to be low and steady with no need of temporarily elevated Cr transport capacity.

On the other hand, Cr transport might be upregulated, i.e., after food ingestion. It was reported that subjects ingesting Cr together with carbohydrates attained far higher muscle Cr levels (18, 19, 49), and studies investigating the effects of insulin in vivo on plasma and muscle Cr accumulation could demonstrate that insulin can enhance muscle Cr accumulation in humans but only when present at physiologically high or supraphysiological concentrations (60). Therefore, we examined the response to various carbohydrates as well as to insulin of Cr uptake into giant sarcolemmal vesicles (Table 1) but were unable to detect significant changes in Cr transport activity in vitro, indicating that these observations are due to secondary or regulatory effects taking place in vivo and that Cr transport is apparently not directly regulated by insulin or the presence of carbohydrates, at least under the conditions used.

The amino acid sequence of the CRT contains several consensus PKC phosphorylation sites (42). Previous work on transfected oocytes transiently expressing CRT demonstrated a dose-dependent decrease in Cr transport activity in the presence of the PKC activator PMA (9). In contrast to the observation with *Xenopus* oocytes, the Cr uptake in Ltk cells transiently expressing a human CRT clone was only slightly inhibited by PMA (42). Our experiments with giant vesicles from skeletal muscle demonstrated that PMA had no significant effect on Cr transport activity compared with preparations treated with the inactive analog 4α-phorbol 12,13-didecanoate (Table 1), indicating that, in rat skeletal muscle, CRT activity might be regulated by a different mechanism or, alternatively, that the enzymes involved in this signaling cascade may have been lost during isolation of the giant vesicles.

It has been shown that caffeine supplementation attenuated the ergogenic effect of Cr supplementation in vivo compared with Cr supplementation alone (67). This has been attributed to increased intramuscular PCr levels. Here, we were able to show that caffeine does not influence CRT function directly, at least in vitro, and that the observed higher PCr levels are rather caused by a shift of the Cr/PCr equilibrium.

Expression of CRT polypeptide species in different tissues. Most tissues in the human organism rely on the uptake of Cr from the extracellular space, especially the metabolically most active tissues with high and fluctuating energy metabolism such as heart, brain, and skeletal muscle, where the highest intracellular Cr concentrations are found (71, 74). Other tissues, such as kidney, intestine, and lung, contain lower levels of Cr due to their lower and more continuous energy turnover (73). Nevertheless, these latter tissues still contain millimolar concentrations of Cr and should therefore also express certain amounts of CRT in their plasma membranes. The CRT peptide chain in rat, rabbit, and human contains 635 amino acids (21, 42, 55), with a calculated molecular mass of 70.6 kDa. Consequently, antisera directed against synthetic peptides corresponding to the NH_2- and COOH-terminal regions of the polypeptide chain, prepared as described earlier (20), should recognize a protein of ~70 kDa on Western blots. Figure 4*A* shows an anti-CRT immunoblot where both antisera consistently immunodetected two protein bands with molecular masses of 55 and 70 kDa. In heart and brain, CRT expression seems to correlate roughly with the well documented high total Cr content as well as with the elevated CK activity in these tissues (71, 74) and reflects their increased energetic requirements (72). In kidney, on the other hand, PCr content and CK activity reach only ~5 and 20%, respectively, of those found in brain and muscle (73). The prominent expression of CRT in kidney might therefore hint at the physiological role of a CRT in kidney that is probably responsible for the recovery of Cr from the urine by the kidney tubules. As expected, lung, testis, and intestine show lower levels of CRT expression. The tissue-specific expression of CRT mRNA by Northern blot hybridization has been investigated previously, and CRT mRNA expression was also detected in most tissues tested but most prominently in kidney, heart, and brain (21, 42, 52, 59), in agreement with CRT protein expression in these tissues shown in Fig. 4*A*. In disagreement with the re-

sults obtained on immunoblots with anti-CRT antibodies, Northern blots showed that mRNA synthesis is apparently absent in human and rabbit liver (21, 42). However, experimental evidence for the presence of a CRT in rat liver comes from the fact that perfused liver from transgenic mice, expressing rat cytosolic brain-type (B)-CK in this organ, can accumulate intracellular concentrations of Cr and PCr of 25 and 8 mM, respectively, at a Cr concentration of 2 mM in the perfusion medium (6). This suggests either that a mechanism for the accumulation of Cr also exists in normal liver or that expression of CK and/or accumulation of Cr in transgenic liver are regulatory signals that stimulate expression of a CRT.

Northern blot analysis also demonstrated the differential expression of two CRT mRNAs in various tissues, which was interpreted to arise from alternative polyadenylation (52) or, more likely, arise from differential splicing, as suggested earlier (20). In agreement with the latter interpretation, our results show the expression of more than one gene product in all tissues tested. Because both the smaller 55-kDa and the 70-kDa CRT proteins share identical NH_2 and COOH termini, they are more likely representing alternatively spliced variants of the CRT, missing one or more of the exons 2 to 12. The existence of a CRT mRNA splice variant missing exon 5 could indeed be confirmed by molecular genetics studies using RACE methods (23).

A third protein band of 116 kDa is often recognized in heart and, to a lesser extent, in skeletal muscle by both of our anti-CRT antibodies. Because the intensity of this latter band is rather variable, we believe that it might represent a dimer of the 55- and/or 70-kDa polypeptide or that it could be the result of membrane protein aggregation, because its presence was sensitive to the extraction procedure and the detergent used (results not shown).

Differential subcellular localization of CRT polypeptide species. The transport studies with giant sarcolemmal vesicles described here clearly confirm the presence of a specific transport system for Cr in the sarcolemma. Thus CRT protein should be highly enriched in purified plasma membrane vesicles and, as judged from the strong signal of anti-CRT immunoblots in total extracts from skeletal muscle (Fig. 4*A*), CRT should be easily detected by anti-CRT antibodies on Western blots. In contrast to our expectations, the immunoreactive signal of the 55- and 70-kDa proteins was almost absent in these highly purified giant sarcolemma vesicle preparations, whereas a rather weak ~58-kDa polypeptide appeared that was enriched in these very preparations. Thus, in contrast to the general opinion, the previously identified CRT proteins of 70 and 55 kDa (20, 41, 43, 66) are apparently not plasma membrane proteins. Seemingly, the sarcolemma contains a different CRT species being expressed in only minor amounts corresponding to the relatively low V_{max} value for Cr transport measured.

This result was confirmed by a surface biotinylation study from cardiac myocytes, which also shows a third polypeptide band at ~58 kDa that binds to the streptavidin beads and is indeed located in the plasma membrane. Because neither the 55- nor the 70-kDa band was detected in the captured biotinylated protein, we believe that these forms of the protein are not expressed on the surface of cardiac myocytes but instead reside at intracellular locations. This result is in agreement with a recent cell surface biotinylation study on C_2C_{12} myotubes (66), which, by use of a different CRT antibody, independently detected similar size (~54 and ~75 kDa) immunoreactive bands in total muscle cell extracts with a weak intermediary protein band of ~58 kDa. In their cell surface biotinylation study, only one band could be enriched in the captured biotinylated proteins, which led the authors of that study to conclude that the other proteins are not expressed on the cell surface, but no conclusions could be given as to their intracellular locations.

Here, we have provided evidence that these proteins are located in mitochondria, since highly purified mitochondria, after density gradient purification, showed an enrichment of the two major CRT species at 55 and 70 kDa. This observation is fully in line with the fact that slow, type I oxidative muscle fibers stained consistently stronger with anti-CRT antibodies compared with fast, type II glycolytic fibers (41), since the mitochondrial content and volume fraction in type I muscle fibers are significantly higher than in type II muscle fibers and highest in cardiac muscle.

To corroborate this finding, erythrocytes, which have been shown to possess an active Cr transport system (2) but do not contain mitochondria, were probed for CRT expression. We found that mouse erythrocytes express only a single ~58-kDa polypeptide form of the CRT, as seen in the captured biotinylated protein and in the plasma membrane vesicles used for transport studies. There is no sign of the existence of polypeptides at 55 or 70 kDa, supporting the hypothesis that the ~58-kDa species is an independent plasma membrane-specific form of the CRT and that the major CRT species are located in mitochondria. This latter assumption was clearly confirmed by indirect immunofluorescence labeling of cultured ARC as well as by cross sections of rat soleus, with anti-CRT antibodies that evidently co-localized with the signals of antibodies directed against the mitochondrial marker proteins ANT, VDAC, and COX (Fig. 7, *A-H*). We cannot exclude a faint additional plasma membrane staining overlapping with the subsarcolemmal mitochondria, which should arise from the weak ~58-kDa immunoreactive CRT band that is visualized by Western blots of highly enriched sarcolemma membranes (Fig. 4*B, lane V*). But it becomes clear that the major fraction of the intracellular signal arises from mitochondria, which are the major compartment of CRT protein localization.

It is tempting to speculate whether there is indeed a functional isoform of CRT within mitochondria, and we are presently investigating this question. From recent data obtained with chemically skinned muscle fibers, no additional release of Cr was observed after incubation of such skinned fibers with strong detergents that

dissolve mitochondria (40). These results were taken to indicate that there was no mitochondrial or other membrane-contained Cr compartment. However, it seems entirely conceivable that Cr is lost very quickly from nonenergized mitochondria (76), e.g., during the rather lengthy skinning procedure, and that this would explain why no additional Cr could be released by permeabilizing the mitochondria. In light of the current discussion about a possible intracellular compartmentation of Cr and PCr pools that have been identified by biochemical fractionation studies (58), by in vivo [^{14}C]PCr/Cr isotope tracer measurements (24), as well as by in vivo nuclear magnetic resonance studies of human skeletal muscle (33), our data offer an explanation for the existence of a Cr and/or PCr pool in mitochondria that is controlled by mitochondrial CRTs. Thus the exact localization and characterization of these new mitochondrial CRT-related proteins, as well as the regulation of mitochondrial Cr transport, seem to deserve our full attention. This holds especially true with respect to the recently discovered clinical manifestation of a new Cr deficiency syndrome that is based on a genetic defect in CRT (51).

We thank Drs. Paolo Bernardi, Max Dolder, Thorsten Hornemann, and Uwe Schlattner for continuous interest in this work and for support and discussion. Special thanks go to Dr. Hans M. Eppenberger for providing adult rat cardiomyocyte cell cultures, and Els Zanolla for technical assistance with the immunofluorescence work.

This study was supported by the Swiss Society for Muscle Diseases (to O. Speer and T. Wallimann), Eidgenössische Technische Hochschule-Zurich (to B. Walzel), the Swiss National Science Foundation (Grant No. 31–62024.00 to T. Wallimann), and the Danish National Research Foundation Grant No. 504–14 (to E. A. Richter).

A part of this work has been published in abstract form: Walzel B, Straumann N, Hornemann T, Magyar J, Kay L, Kristiansen S, Richter EA, and Wallimann T. A new mitochondrial transporter: active creatine transport into mitochondria. *Eur J Med Res* 5, *Suppl* 1: 28–29, 2000.

Present address of J. P. Magyar: MyoContract Pharmaceutical Research Ltd., Biocenter Basel, Klingelbergstrasse 70, CH-4056 Basel, Switzerland.

REFERENCES

1. **Barth PG, Scholte HR, Berden JA, Van der Klei-Van Moorsel JM, Luyt-Houwen IE, Van 't Veer-Korthof ET, Van der Harten JJ, and Sobotka-Plojhar MA**. An X-linked mitochondrial disease affecting cardiac muscle, skeletal muscle and neutrophil leucocytes. *J Neurol Sci* 62: 327–355, 1983.
2. **Bennett SE, Bevington A, and Walls J.** Regulation of intracellular creatine in erythrocytes and myoblasts: influence of uraemia and inhibition of Na,K-ATPase. *Cell Biochem Funct* 12: 99–106, 1994.
3. **Bergnes G, Yuan W, Khandekar VS, O'Keefe MM, Martin KJ, Teicher BA, and Kaddurah-Daouk R.** Creatine and phosphocreatine analogs: anticancer activity and enzymatic analysis. *Oncol Res* 8: 121–130, 1996.
4. **Bolhuis PA, Hensels GW, Hulsebos TJ, Baas F, and Barth PG.** Mapping of the locus for X-linked cardioskeletal myopathy with neutropenia and abnormal mitochondria (Barth syndrome) to Xq28. *Am J Hum Genet* 48: 481–485, 1991.
5. **Brdiczka D, Pette D, Brunner G, and Miller F.** Compartmental dispersion of enzymes in rat liver mitochondria. *Eur J Biochem* 5: 294–304, 1968.
6. **Brosnan MJ, Halow JM, and Koretsky AP.** Manipulating creatine kinase activity in transgenic mice to study control of energy metabolism. *Biochem Soc Trans* 19: 1010–1014, 1991.
7. **Carter AJ, Muller RE, Pschorn U, and Stransky W.** Preincubation with creatine enhances levels of creatine phosphate and prevents anoxic damage in rat hippocampal slices. *J Neurochem* 64: 2691–2699, 1995.
8. **Constantin-Teodosiu D, Greenhaff PL, Gardiner SM, Randall MD, March JE, and Bennett T.** Attenuation by creatine of myocardial metabolic stress in Brattleboro rats caused by chronic inhibition of nitric oxide synthase. *Br J Pharmacol* 116: 3288–3292, 1995.
9. **Dai W, Vinnakota S, Qian X, Kunze DL, and Sarkar HK.** Molecular characterization of the human CRT-1 creatine transporter expressed in Xenopus oocytes. *Arch Biochem Biophys* 361: 75–84, 1999.
10. **Daniels GM and Amara SG.** Selective labeling of neurotransmitter transporters at the cell surface. *Methods Enzymol* 296: 307–318, 1998.
11. **Dengler R, Hofmann WW, and Rudel R.** Effects of potassium depletion and insulin on resting and stimulated skeletal rat muscle. *J Neurol Neurosurg Psychiatry* 42: 818–826, 1979.
12. **Earnest CP, Almada AL, and Mitchell TL.** High-performance capillary electrophoresis—pure creatine monohydrate reduces blood lipids in men and women. *Clin Sci (Colch)* 91: 113–118, 1996.
13. **Eichler EE, Lu F, Shen Y, Antonacci R, Jurecic V, Doggett NA, Moyzis RK, Baldini A, Gibbs RA, and Nelson DL.** Duplication of a gene-rich cluster between 16p11.1 and Xq28: a novel pericentromeric-directed mechanism for paralogous genome evolution. *Hum Mol Genet* 5: 899–912, 1996.
14. **Eppenberger-Eberhardt M, Flamme I, Kurer V, and Eppenberger HM.** Reexpression of alpha-smooth muscle actin isoform in cultured adult rat cardiomyocytes. *Dev Biol* 139: 269–278, 1990.
15. **Eppenberger-Eberhardt M, Riesinger I, Messerli M, Schwarb P, Muller M, Eppenberger HM, and Wallimann T.** Adult rat cardiomyocytes cultured in creatine-deficient medium display large mitochondria with paracrystalline inclusions, enriched for creatine kinase. *J Cell Biol* 113: 289–302, 1991.
16. **Fitch CD and Chevli R.** Inhibition of creatine and phosphocreatine accumulation in skeletal muscle and heart. *Metabolism* 29: 686–690, 1980.
17. **Gordon A, Hultman E, Kaijser L, Kristjansson S, Rolf CJ, Nyquist O, and Sylven C.** Creatine supplementation in chronic heart failure increases skeletal muscle creatine phosphate and muscle performance. *Cardiovasc Res* 30: 413–418, 1995.
18. **Green AL, Hultman E, Macdonald IA, Sewell DA, and Greenhaff PL.** Carbohydrate ingestion augments skeletal muscle creatine accumulation during creatine supplementation in humans. *Am J Physiol Endocrinol Metab* 271: E821–E826, 1996.
19. **Green AL, Simpson EJ, Littlewood JJ, Macdonald IA, and Greenhaff PL.** Carbohydrate ingestion augments creatine retention during creatine feeding in humans. *Acta Physiol Scand* 158: 195–202, 1996.
20. **Guerrero-Ontiveros ML and Wallimann T.** Creatine supplementation in health and disease. Effects of chronic creatine ingestion in vivo: down-regulation of the expression of creatine transporter isoforms in skeletal muscle. *Mol Cell Biochem* 184: 427–437, 1998.
21. **Guimbal C and Kilimann MW.** A Na(+)-dependent creatine transporter in rabbit brain, muscle, heart, and kidney. cDNA cloning and functional expression. *J Biol Chem* 268: 8418–8421, 1993.
22. **Heinanen K, Nanto-Salonen K, Komu M, Erkintalo M, Alanen A, Heinonen OJ, Pulkki K, Nikoskelainen E, Sipila I, and Simell O.** Creatine corrects muscle 31P spectrum in gyrate atrophy with hyperornithinaemia. *Eur J Clin Invest* 29: 1060–1065, 1999.
23. **Henry HO, Speer O, Braissant B, Eilers C, Bachmann A, and Wallimann T.** Expression of splice variants of the creatine transporter in the rat brain, muscle, and kidney (Abstract). *Cell Biol Int* 25: 940, 2001.
24. **Hochachka PW and Mossey MK.** Does muscle creatine phosphokinase have access to the total pool of phosphocreatine plus creatine? *Am J Physiol Regulatory Integrative Comp Physiol* 274: R868–R872, 1998.
25. **Hoosein NM, Martin KJ, Abdul M, Logothetis CJ, and Kaddurah-Daouk R.** Antiproliferative effects of cyclocreatine

on human prostatic carcinoma cells. *Anticancer Res* 15: 1339–1342, 1995.
26. **Ingwall JS.** Creatine and the control of muscle-specific protein synthesis in cardiac and skeletal muscle. *Circ Res* 38: 115–123, 1976.
27. **Iyer GS, Krahe R, Goodwin LA, Doggett NA, Siciliano MJ, Funanage VL, and Proujansky R.** Identification of a testis-expressed creatine transporter gene at 16p11.2 and confirmation of the X-linked locus to Xq28. *Genomics* 34: 143–146, 1996.
28. **Juel C.** Human muscle lactate transport can be studied in sarcolemmal giant vesicles made from needle-biopsies. *Acta Physiol Scand* 142: 133–134, 1991.
29. **Juel C, Kristiansen S, Pilegaard H, Wojtaszewski J, and Richter EA.** Kinetics of lactate transport in sarcolemmal giant vesicles obtained from human skeletal muscle. *J Appl Physiol* 76: 1031–1036, 1994.
30. **Klivenyi P, Ferrante RJ, Matthews RT, Bogdanov MB, Klein AM, Andreassen OA, Mueller G, Wermer M, Kaddurah-Daouk R, and Beal MF.** Neuroprotective effects of creatine in a transgenic animal model of amyotrophic lateral sclerosis. *Nat Med* 5: 347–350, 1999.
31. **Klopstock T, Querner V, Schmidt F, Gekeler F, Walter M, Hartard M, Henning M, Gasser T, Pongratz D, Straube A, Dieterich M, and Muller-Felber W.** A placebo-controlled crossover trial of creatine in mitochondrial diseases. *Neurology* 55: 1748–1751, 2000.
32. **Kornacker M, Schlattner U, Wallimann T, Verneris MR, Negrin RS, Kornacker B, Staratschek-Jox A, Diehl V, and Wolf J.** Hodgkin disease-derived cell lines expressing ubiquitous mitochondrial creatine kinase show growth inhibition by cyclocreatine treatment independent of apoptosis. *Int J Cancer* 94: 513–519, 2001.
33. **Kreis R, Jung B, Slotboom J, Felblinger J, and Boesch C.** Effect of exercise on the creatine resonances in 1H MR spectra of human skeletal muscle. *J Magn Reson* 137: 350–357, 1999.
34. **Kristiansen S, Hargreaves M, and Richter EA.** Exercise-induced increase in glucose transport, GLUT-4, and VAMP-2 in plasma membrane from human muscle. *Am J Physiol Endocrinol Metab* 270: E197–E201, 1996.
35. **Lillie JW, O'Keefe M, Valinski H, Hamlin HA Jr, Varban ML, and Kaddurah-Daouk R.** Cyclocreatine (1-carboxymethyl-2-iminoimidazolidine) inhibits growth of a broad spectrum of cancer cells derived from solid tumors. *Cancer Res* 53: 3172–3178, 1993.
36. **Martin KJ, Vassallo CD, Teicher BA, and Kaddurah-Daouk R.** Microtubule stabilization and potentiation of taxol activity by the creatine analog cyclocreatine. *Anticancer Drugs* 6: 419–426, 1995.
37. **Martin KJ, Winslow ER, and Kaddurah-Daouk R.** Cell cycle studies of cyclocreatine, a new anticancer agent. *Cancer Res* 54: 5160–5165, 1994.
38. **Matthews PM, Allaire C, Shoubridge EA, Karpati G, Carpenter S, and Arnold DL.** In vivo muscle magnetic resonance spectroscopy in the clinical investigation of mitochondrial disease. *Neurology* 41: 114–120, 1991.
39. **Matthews RT, Yang L, Jenkins BG, Ferrante RJ, Rosen BR, Kaddurah-Daouk R, and Beal MF.** Neuroprotective effects of creatine and cyclocreatine in animal models of Huntington's disease. *J Neurosci* 18: 156–163, 1998.
40. **Menin L, Panchichkina M, Keriel C, Olivares J, Braun U, Seppet EK, and Saks VA.** Macrocompartmentation of total creatine in cardiomyocytes revisited. *Mol Cell Biochem* 220: 149–159, 2001.
41. **Murphy R, McConell G, Cameron-Smith D, Watt K, Ackland L, Walzel B, Wallimann T, and Snow R.** Creatine transporter protein content, localization, and gene expression in rat skeletal muscle. *Am J Physiol Cell Physiol* 280: C415–C422, 2001.
42. **Nash SR, Giros B, Kingsmore SF, Rochelle JM, Suter ST, Gregor P, Seldin MF, and Caron MG.** Cloning, pharmacological characterization, and genomic localization of the human creatine transporter. *Receptors Channels* 2: 165–174, 1994.
43. **Neubauer S, Remkes H, Spindler M, Horn M, Wiesmann F, Prestle J, Walzel B, Ertl G, Hasenfuss G, and Wallimann T.** Downregulation of the Na(+)-creatine cotransporter in failing human myocardium and in experimental heart failure. *Circulation* 100: 1847–1850, 1999.
44. **Osbakken M, Ito K, Zhang D, Ponomarenko I, Ivanics T, Jahngen EG, and Cohn M.** Creatine and cyclocreatine effects on ischemic myocardium: 31P nuclear magnetic resonance evaluation of intact heart. *Cardiology* 80: 184–195, 1992.
45. **Passaquin AC, Renard M, Kay L, Challet C, Mokhtarian A, Wallimann T, and Ruegg UT.** Creatine supplementation reduces skeletal muscle degeneration and enhances mitochondrial function in mdx mice. *Neuromuscul Disord* 12: 174–182, 2002.
46. **Ploug T, Wojtaszewski J, Kristiansen S, Hespel P, Galbo H, and Richter EA.** Glucose transport and transporters in muscle giant vesicles: differential effects of insulin and contractions. *Am J Physiol Endocrinol Metab* 264: E270–E278, 1993.
47. **Powell T and Noma A.** *Isolation and Culture of Adult Cardiac Myocytes*. London, UK: *Academic*, 1998.
48. **Pulido SM, Passaquin AC, Leijendekker WJ, Challet C, Wallimann T, and Ruegg UT.** Creatine supplementation improves intracellular Ca2+ handling and survival in mdx skeletal muscle cells. *FEBS Lett* 439: 357–362, 1998.
49. **Robinson TM, Sewell DA, Hultman E, and Greenhaff PL.** Role of submaximal exercise in promoting creatine and glycogen accumulation in human skeletal muscle. *J Appl Physiol* 87: 598–604, 1999.
50. **Rojo M and Wallimann T.** The mitochondrial ATP/ADP carrier: interaction with detergents and purification by a novel procedure. *Biochim Biophys Acta* 1187: 360–367, 1994.
51. **Salomons GS, van Dooren SJ, Verhoeven NM, Cecil KM, Ball WS, Degrauw TJ, and Jakobs C.** X-linked creatine-transporter gene (SLC6A8) defect: a new creatine-deficiency syndrome. *Am J Hum Genet* 68: 1497–1500, 2001.
52. **Saltarelli MD, Bauman AL, Moore KR, Bradley CC, and Blakely RD.** Expression of the rat brain creatine transporter in situ and in transfected HeLa cells. *Dev Neurosci* 18: 524–534, 1996.
53. **Schimmel L, Khandekar VS, Martin KJ, Riera T, Honan C, Shaw DG, and Kaddurah-Daouk R.** The synthetic phosphagen cyclocreatine phosphate inhibits the growth of a broad spectrum of solid tumors. *Anticancer Res* 16: 375–380, 1996.
54. **Schlattner U, Möckli N, Speer O, Werner S, and Wallimann T.** Creatine kinase and creatine transporter in normal, wounded and diseased skin. *J Invest Dermatol* 118: 416–423, 2002.
55. **Schloss P, Mayser W, and Betz H.** The putative rat choline transporter CHOT1 transports creatine and is highly expressed in neural and muscle-rich tissues. *Biochem Biophys Res Commun* 198: 637–645, 1994.
56. **Sipila I, Rapola J, Simell O, and Vannas A.** Supplementary creatine as a treatment for gyrate atrophy of the choroid and retina. *N Engl J Med* 304: 867–870, 1981.
57. **Smith PB and Appel SH.** Isolation and characterization of the surface membranes of fast and slow mammalian skeletal muscle. *Biochim Biophys Acta* 466: 109–122, 1977.
58. **Soboll S, Conrad A, Eistert A, Herick K, and Kramer R.** Uptake of creatine phosphate into heart mitochondria: a leak in the creatine shuttle. *Biochim Biophys Acta* 1320: 27–33, 1997.
59. **Sora I, Richman J, Santoro G, Wei H, Wang Y, Vanderah T, Horvath R, Nguyen M, Waite S, Roeske WR, and Yamamura HI.** The cloning and expression of a human creatine transporter. *Biochem Biophys Res Commun* 204: 419–427, 1994.
60. **Steenge GR, Lambourne J, Casey A, Macdonald IA, and Greenhaff PL.** Stimulatory effect of insulin on creatine accumulation in human skeletal muscle. *Am J Physiol Endocrinol Metab* 275: E974–E979, 1998.
61. **Stephan MM, Chen MA, Penado KM, and Rudnick G.** An extracellular loop region of the serotonin transporter may be involved in the translocation mechanism. *Biochemistry* 36: 1322–1328, 1997.
62. **Tarnopolsky M and Martin J.** Creatine monohydrate increases strength in patients with neuromuscular disease. *Neurology* 52: 854–857, 1999.
63. **Tarnopolsky MA, Parshad A, Walzel B, Schlattner U, and Wallimann T.** Creatine transporter and mitochondrial creatine

kinase protein content in myopathies. *Muscle Nerve* 24: 682–688, 2001.
64. **Tarnopolsky MA, Roy BD, and MacDonald JR.** A randomized, controlled trial of creatine monohydrate in patients with mitochondrial cytopathies. *Muscle Nerve* 20: 1502–1509, 1997.
65. **Terjung RL, Clarkson P, Eichner ER, Greenhaff PL, Hespel PJ, Israel RG, Kraemer WJ, Meyer RA, Spriet LL, Tarnopolsky MA, Wagenmakers AJ, and Williams MH.** American College of Sports Medicine Roundtable. The physiological and health effects of oral creatine supplementation. *Med Sci Sports Exerc* 32: 706–717, 2000.
66. **Tran TT, Dai W, and Sarkar HK.** Cyclosporin A inhibits creatine uptake by altering surface expression of the creatine transporter. *J Biol Chem* 275: 35708–35714, 2000.
67. **Vandenberghe K, Gillis N, Van Leemputte M, Van Hecke P, Vanstapel F, and Hespel P.** Caffeine counteracts the ergogenic action of muscle creatine loading. *J Appl Physiol* 80: 452–457, 1996.
68. **Vannas-Sulonen K, Sipila I, Vannas A, Simell O, and Rapola J.** Gyrate atrophy of the choroid and retina. A five-year follow-up of creatine supplementation. *Ophthalmology* 92: 1719–1727, 1985.
69. **Vary TC and Neely JR.** Sodium dependence of carnitine transport in isolated perfused adult rat hearts. *Am J Physiol Heart Circ Physiol* 244: H247–H252, 1983.
70. **Walker JB.** Creatine: biosynthesis, regulation, and function. *Adv Enzymol Relat Areas Mol Biol* 50: 177–242, 1979.
71. **Wallimann T.** Bioenergetics. Dissecting the role of creatine kinase. *Curr Biol* 4: 42–46, 1994.
72. **Wallimann T, Dolder M, Schlattner U, Eder M, Hornemann T, Kraft T, and Stolz M.** Creatine kinase: an enzyme with a central role in cellular energy metabolism. *MAGMA* 6: 116–119, 1998.
73. **Wallimann T and Hemmer W.** Creatine kinase in non-muscle tissues and cells. *Mol Cell Biochem* 133–134: 193–220, 1994.
74. **Wallimann T, Wyss M, Brdiczka D, Nicolay K, and Eppenberger HM.** Intracellular compartmentation, structure and function of creatine kinase isoenzymes in tissues with high and fluctuating energy demands: the "phosphocreatine circuit" for cellular energy homeostasis. *Biochem J* 281: 21–40, 1992.
75. **Walter MC, Lochmuller H, Reilich P, Klopstock T, Huber R, Hartard M, Hennig M, Pongratz D, and Muller-Felber W.** Creatine monohydrate in muscular dystrophies: a double-blind, placebo-controlled clinical study. *Neurology* 54: 1848–1850, 2000.
76. **Walzel B, Boehm E, Speer O, Kristiansen S, Richter EA, and Wallimann T.** Novel creatine transporter (CRT) isoforms: a minor species in plasma membrane vesicles and two major species in mitochondria (Abstract). *Cell Biol Int* 25: 949, 2001.
77. **Wyss M and Kaddurah-Daouk R.** Creatine and creatinine metabolism. *Physiol Rev* 80: 1107–1213, 2000.